where all the integrals involved in the above expression are analytical. The eigenvalue condition is given by

$$\frac{[\bar{J}_0(U) - \bar{J}_0(\bar{U}][\bar{K}_0(Wc) - \bar{Y}_0(\bar{U}c)]}{[\bar{J}_0(U) - \bar{Y}_0(\bar{U})][\bar{K}_0(Wc) - \bar{J}_0(\bar{U}c)]} = \frac{J_1(\bar{U}c)Y_1(\bar{U})}{J_1(\bar{U})Y_1(\bar{U}c)}, \quad (9)$$

where $c = (a_{cl}/a_{co})$ and $\bar{Z}_m(x) = (Z_m(x))/(xZ_{m+1}(x))$ (Z represents the Bessel functions J, Y, or K).

The analytical expression for κ is given as

$$\kappa = \frac{a_{co}}{U_1 - U_n}\frac{k_0}{4}\Delta n^2 A_1 A_n[U_1 J_1(U_1)J_0(U_n) - U_n J_0(U_1)J_1(U_n)], \quad (10)$$

where U_n is the value of U corresponding to the LP_{0n} mode, and A_1 and A_n are the corresponding normalisation constants.

REFERENCES

1. A.M. Vengsarkar, P.J. Lemaire, J.B. Judkins, V. Bhatia, T. Erdogan, and J.E. Sipe, Long period fiber gratings as band-rejection filters, J Lightwave Technol 14 (1996), 58–64.
2. P.D. Greene and H.N. Rourke, Tailoring long period optical fiber gratings fot flattening EDFA gain spectra, Electron Lett 35 (1999), 1373–1374.
3. V. Bhatia and A.M. Vengsarkar, Optical fiber long period grating sensors, Opt Lett 21 (1996), 692–694.
4. B.H. Lee, Y. Liu, S.B. Lee, S.S. Choi, and J.N. Jang, Displacements of the resonant peaks of a long period fiber grating induced by a change of ambient refractive index, Opt Lett 22 (1997), 1769–1771.
5. H.J. Patrick, A.D. Kersey, and F. Bucholtz, Analysis of the response of long period fiber gratings to external index of refraction, J Lightwave Technol 16 (1998), 1606–1612.
6. M.J. Adams, An Introduction to Optical Waveguides, Wiley Interscience, New York, 1981, pp. 223–233.
7. A.J. Fielding, K. Edinger, and C.C. Davis, Experimental observation of mode evolution in single-mode tapered optical fibers, J Lightwave Technol 17 (1999), 1649–1656.
8. T. Erdogan, Cladding-mode resonances in short- and long-period fiber grating filters, J Opt Soc Am A14 (1997), 1760–1773.
9. R. Kashyap, Theory of Fiber Bragg Gratings, Academic Press, London, 1999, pp. 171–174.
10. X. Shu, X. Zhu, S. Jiang, W. Shi, and D. Huang, High sensitivity of dual resonant peaks of long period fiber grating to surrounding refractive index changes, Electron Lett 35 (1999), 1580–1581.
11. Sunanda and E.K. Sharma, Field variational analysis for modal gain in erbium-doped fiber amplifiers, J Opt Soc Am B16 (1999), 1344–1347.
12. R. Singh, Sunanda, and E.K. Sharma, Propagation characteristics of single mode optical fibers with arbitrary complex index profiles: A direct numerical approach, J Quantum Electron 37 (2001), 635–639.
13. E. Desurvire, Erbium Doped Fiber Amplifiers, Wiley, New York, 1994, p. 252.
14. M. Monerie, Propagation in doubly clad single mode fibers, IEEE Trans Microwave Theory Tech 30 (1982), 381–388.

HIGH PERFORMANCE RF INTEGRATED PASSIVE DEVICES ON THICK OXIDE SUBSTRATE USING Cu-BCB PROCESS

Inho Jeong,[1] Ki-Joong Kim,[1] Tong-Ook Kong,[1] Jun-Seok Kim,[1] Hyung-Kyu Choi,[1] Choong-Mo Nam,[1] Dong-Wook Kim,[1] and Young-Se Kwon[2]
[1] Telephus Inc.
25-11 Jang-dong, Yuseong-gu
Taejeon, 305-343, Korea
[2] Dept. of EE, KAIST
373-1 Kusong-dong, Yuseong-gu
305-701, Taejeon, Korea

Received 18 September 2002

ABSTRACT: *In this paper, we develop a low-cost manufacturing technology for RF substrate and a high-performance process technology for integrated passive devices by electrochemically forming thick oxide on Si wafer and processing Cu thick metal and BCB. Several integrated passive devices such as LPF, BPF, and balun are fabricated using this technology and they show good RF performance in spite of their small chip size.* © 2003 Wiley Periodicals, Inc. Microwave Opt Technol Lett 37: 49–52, 2003; Published online in Wiley InterScience (www.interscience.wiley.com). DOI 10.1002/mop.10821

Key words: *IPD (integrated passive device); LPF; balun; Cu process; BCB; multi-layer RF passive devices*

1. INTRODUCTION

Nowadays, an RF system, which has small volume or size, low cost and multi-functional integration, is one of the most popular topics. But the RF front-end of wireless devices still contain a large amount of discrete components, which is an important obstacle for further size reduction. An RF integrated passive device (RFIPD) whose components are integrated on a substrate has been an attractive option for building wireless modules. In addition, the RFIPD in this work not only reduces the cost and size by eliminating the need for discrete components, but also has been demonstrated to exhibit superior performance for on-chip components.

Of all the passive components in an RF system, the inductors are typically the most difficult to integrate with sufficiently high quality. Inductors are key components required for impedance matching and resonator elements in RF circuits. Obviously, integrated capacitors, resistors, and low-loss interconnects are required to be able to realize small size and high performance in RF systems [1].

Silicon substrate is known to have many advantages, such as inexpensive material, good thermal conductivity, and a stable and mature process technology. But its utilization has been limited in the fast-growing wireless market by large signal loss and signal leakage through parasitic substrate capacitance. So, the insulating property of an SiO_2 layer is used for isolation, and in order to effectively operate this SiO_2 layer in RF applications, it needs to be thick, in order to capacitively isolate it from the underlying conducting Si substrate. To obtain thick oxide on silicon substrate, a porous silicon technique is considered as a potential solution. In porous material, the lattice has a large number of its silicon atoms removed by an electrochemical reaction, thereby producing honeycomb-like structure. Initial work on using porous silicon for RF applications took advantage of the oxidation process of the porous silicon layer [2].

In this paper, we will introduce improved Si substrate technology, called Si smart substrate or thick oxide (TO) Si substrate, and

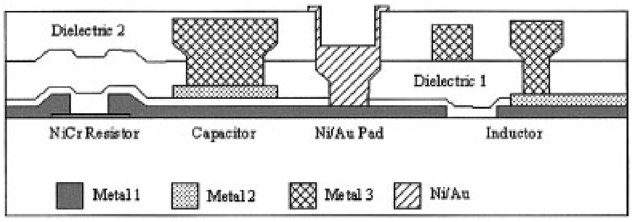

Figure 1 Schematic cross-section of the Cu/BCB process used in this work

a Cu process with a benzo cyclo butene (BCB) interlayer. We will highlight their applicability and need for the realization of low-insertion-loss low-pass filter (LPF) and narrow band-pass filter (BPF), which may be used in wireless telecommunications and WLAN.

2. TECHNOLOGY AND PASSIVE LIBRARY

In this section, we introduce an advanced passive process using thick Cu metal. This process technology is targeted to high performance, low cost, and small sized passive-only circuits, such as filters or baluns. A thick (10-μm) Cu metallization layer and insulated surface of Si (with a 25-μm SiO2 layer on top) make it possible to obtain high RF performance for wireless communication systems and integrated RF modules. BCB, a low-dielectric-constant material, is adapted to reduce parasitic capacitance between metal layers. Precision NiCr resistors and SiN MIM capacitors are also integrated. An electro-plated Ni/Au pad is used for wire-bond interconnection and a Cu pad is used for the wafer-level chip-scale package (WLCSP). In this work, we use 6-in. (150-mm in diameter) wafers for high-volume production.

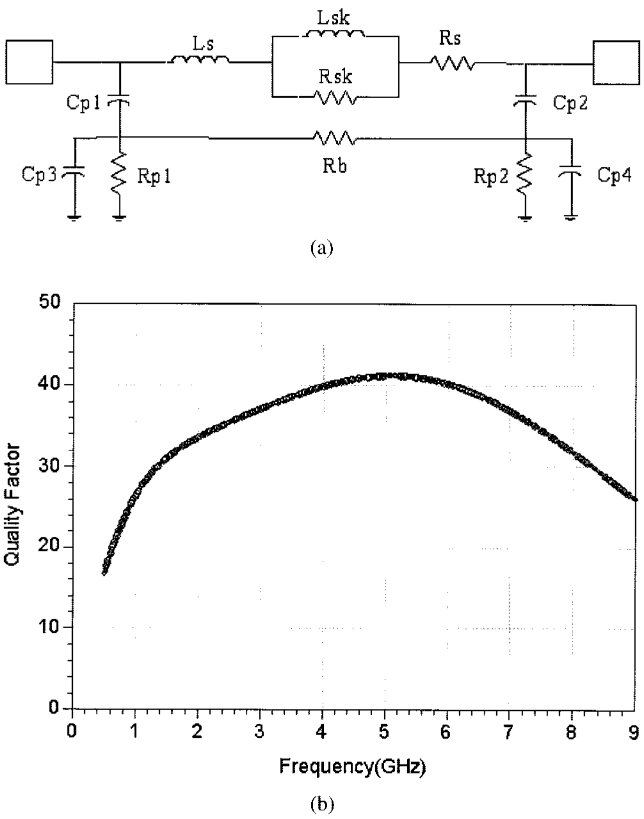

Figure 2 Equivalent circuit model and Q factor of inductor: (a) wide-band equivalent circuit model; (b) quality factor of 2.7-nH spiral inductor

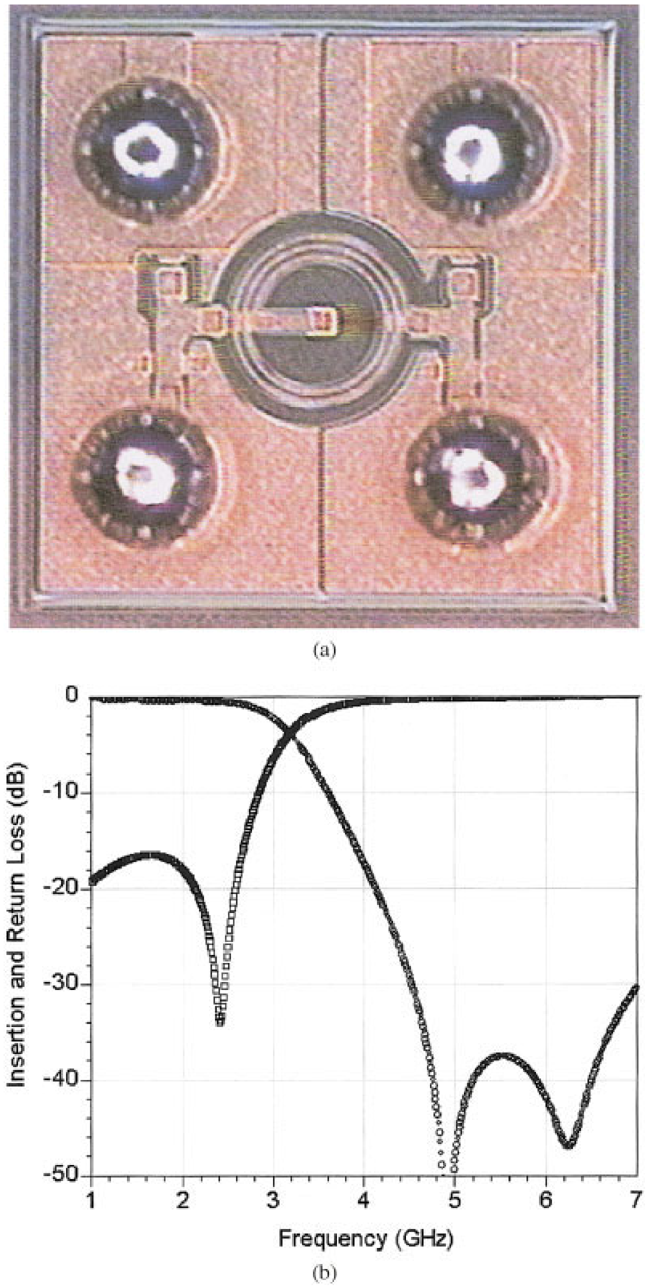

Figure 3 Low-pass filter for WLAN: (a) photograph of the LPF on thick oxide Si substrate; (b) measured insertion and return loss of the LPF [Color figure can be viewed in the online issue, is available at www.interscience.wiley.com.]

2.1. *Substrate and Thin Film Process*

Unlike semi-insulating GaAs or InP, silicon has typically been forced to rely upon the insulating properties of SiO_2 for isolation. This requires a very thick oxide layer to isolate capacitively between devices on Si substrate. The challenge to implementing this thick oxide layer is two-fold. One is silicon substrate shattering due to the difference in thermal expansion coefficients of the oxide layer and Si substrate. The other is cost-effective manufacturing. Basically, the fabrication costs and the time to grow such thick oxide by conventional techniques make the implementation unrealistic. To overcome the limitations of these conventional techniques, we used oxidized porous silicon, which is typically formed in an electrochemical cell using an HF solution and anodization technique.

A uniform oxide layer of 25 μm or greater was made on the whole surface of a 6-in. silicon wafer. The time needed to make this 25-μm oxide layer is less than half an hour. Additionally, we developed a thin film multilayer technology for RF and microwave applications. In this technology, we used 10-μm electroplated Cu metal and BCB dielectric on our smart substrate. Cu metal is an optimal choice for low conductive metal loss and high-speed operation in tough environments. Photosensitive BCB material was used as an interlayer between the first Cu metal and the second Cu plated metal. The photo-BCB has many attractive properties, such as processing compatibility with existing IC manufacturing techniques, low moisture uptake, low cure temperature, rapid thermal curing, high planarization level, low dielectric constant, and so on. The 5-μm BCB layer was used as an interlayer of metal layers and the 8-μm BCB layer was used for final passivation.

NiCr was used for the resistor and SiNx dielectric material was employed as the interlayer insulator of the metal-insulator-metal (MIM) capacitor. A total of two Cu metal layers and one dummy Cu layer were used for NiCr contact, bottom and top metal formation of MIM capacitor, spiral inductor patterning, and element interconnection. An Ni/Au pad was selected for wire bond interconnection, because it can enable the integration of passive-only circuits with other active devices for multi-chip module (MCM) application. In case of direct board-level integration, a thick copper pad is selected for a solder-ball bumped package. Figure 1 shows a schematic cross-sectional view of our thin-film process structure.

2.2. Passive Library

The on-chip inductors, which were one of the major technological challenges, were fabricated using Cu of 10-μm thickness on 6-in. Si smart substrate SiO_2 of 25-μm thickness. They showed a maximum quality factor range of 25–60 or greater, depending on geometrical parameters and inductance values of 0.35–31.5 nH. We measured 96 rectangular spiral inductors (microstrip-like) and 110 circular spiral inductors (CPW structures), and established an inductor library for them. Figure 2(a) shows the equivalent circuit model of spiral inductor made on Si smart substrate. The shunt parasitic results from a combination of thick oxide capacitance ($Cp1$, $Cp2$) and substrate parasitic ($Cp3$, $Cp4$, $Rp1$, $Rp2$, Rb). Rsk and Lsk describe the frequency-dependent series resistance and inductance induced by skin effect and eddy current effect [3]. Figure 2(b) shows the quality factor of CPW circular spiral inductor ($L = 2.7$ nH) with frequency.

A thin silicon-nitride layer is used as the capacitor dielectric, and capacitance density is around 540 pF/mm^2. The breakdown voltage is above 100 V in the case of a 5.4-pF capacitor. Precision NiCr resistors are used for implementation of resistance at RF. This precision resistor has a nominal sheet resistance of 20Ω per square. The resistor width can be determined by current handling capacity. The insertion loss of the 50Ω coplanar transmission line ($W = 50$ μm, $G = 20$ μm) is 0.03 dB/mm at 4 GHz. The transmission line also showed high performance up to more than 10 GHz. The insertion loss was below 0.1 dB/mm up to 15 GHz [4].

3. RF INTEGRATED PASSIVE DEVICES

These thick oxide substrate and RF passive integration technology of MIM capacitors, resistors, and high Q inductors enabled us to realize fully integrated passive functional blocks. Utilizing high quality passive devices, we fabricated several kinds of integrated passive devices, such as low-pass filter, power combiner, fixed attenuator, balun, and so on. These devices could be wafer-level-packaged using a PbSn solder-ball bump. The size and pitch of the bumps are selected so that the device can be placed directly on PWB board via the conventional surface mounting techniques. The solder bumps are a eutectic Sn/Pb alloy and are nominally 0.3 mm in diameter.

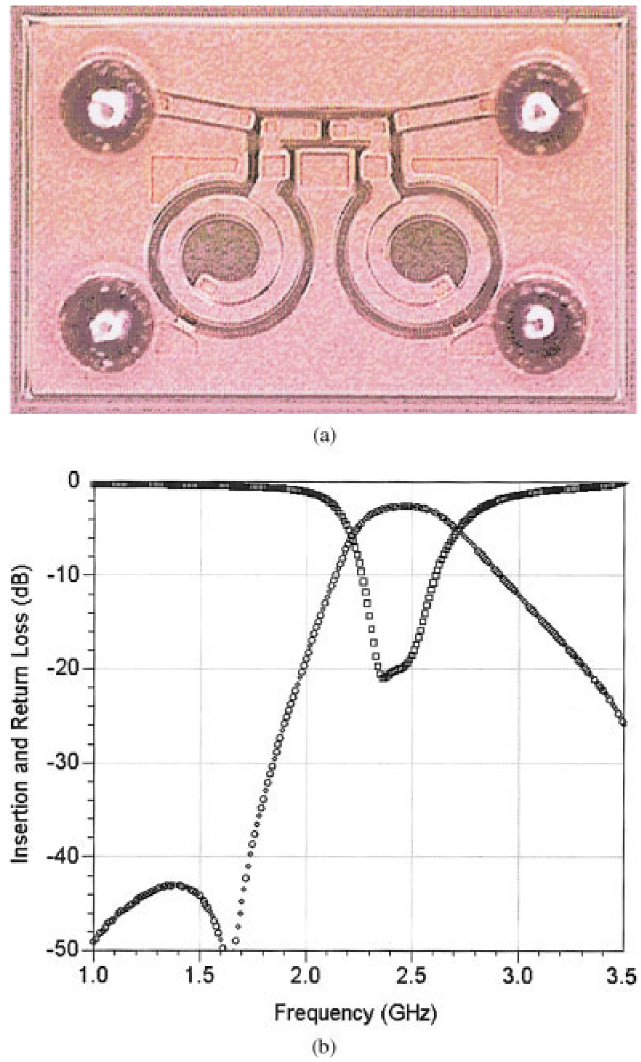

Figure 4 Band-pass filter for WLAN: (a) photograph of the BPF on thick oxide Si substrate; (b) measured insertion and return loss of the BPF [Color figure can be viewed in the online issue, is available at www.interscience.wiley.com.]

3.1. Integrated Low Pass Filter

The filter is very essential component in many electrical circuits. It may be realized by combinations of capacitive and inductive lumped-passive components. These filters may then be integrated on our smart substrate using the Cu-BCB thin film process. Figure 3(a) shows the fabricated LC-type lumped LPF for 2.4-GHz WLAN application. The 300-μm solder ball is attached to a 10-μm thick Cu pad for surface mount on PWB. In Figure 3(b), the network analyzer measurement results of LPF are shown. The insertion loss in pass band (2.4–2.5 GHz) is below 0.5 dB and return loss is below -20 dB. The attenuation in second harmonic

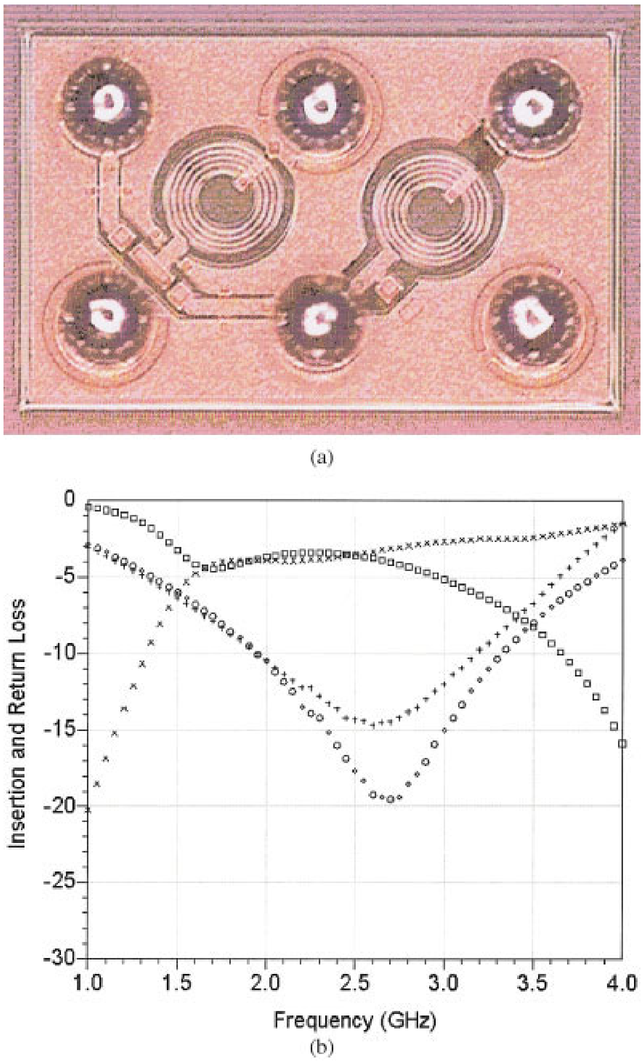

Figure 5 Balun for WLAN: (a) photograph of the Balun on thick oxide Si substrate; (b) measured insertion and return loss of the Balun. (□: insertion loss of 0° port, X: insertion loss of 180° port, ○: return loss of unbalunce port, +: return loss of balunce port) [Color figure can be viewed in the online issue, is available at www.interscience.wiley.com.]

frequency is less than −30 dB, and the size of the LPF is 1.2 mm × 1.2 mm.

3.2. Integrated Narrow Band Pass Filter

For WLNA application, the band-pass filter is fabricated using Cu-BCB and our smart substrate technology. The center frequency of the BPF is 2450 MHz and the pass band's width is 100 MHz. In order to achieve this narrow frequency response, a second order capacitive coupled resonator filter was chosen for realization. The result shown in Figure 4(b) was achieved. Within the pass band, an insertion loss of less than 2.4 dB was measured and, at the edges of the band, the insertion loss was 2.8 dB. From these values, the quality factor of the inductor can be deduced to be on the order of 50. Because of the high value of the Q factor, steep filter skirts were achieved. Within 400-MHz low band from the edge of the band, the insertion loss increases to 20 dB and reaches 40 dB within 650 MHz.

3.3. Integrated Balun

Baluns are important components in front-end systems to couple or divide power from different ports with the same magnitude and phase difference of 180°. Traditionally, transmission lines are used to realize baluns, but the size become too large to make on our substrate. We convert the specific transmission lines into the lumped passive element in order to resolve this size problem. A photograph of the integrated balun using our own technology is shown in Figure 5(a); its size is 1.85 mm × 1.2 mm. Figure 5(b) shows RF performances of 2450-MHz LC-type lumped balun. From 2400 MHz to 2500 MHz, the insertion loss of the balun was just about 0.5 dB and only the phase difference deviates less than 3° and amplitude imbalance was less than 0.3 dB.

3.4. Other RFIPDs

In addition to LPF, BPF, and balun, we developed some other RFIPDs on smart substrate. These devices are LPFs and baluns for 900 MHz, 1800 MHz, and 5200 MHz; diplexer for GSM/DCS dual band; power divider for 900 MHz and 1800 MHz; fixed attenuators; and so on. The insertion loss of power combiner for 1800 MHz was about 0.6 dB, the return loss was less than −15 dB, and port isolation was greater than 20 dB. In the case of LPFs, the insertion losses are about 0.5 dB for 900 MHz, 1800 MHz, and 5200 MHz. The diplexer for GSM/DCS shows 0.5-dB insertion loss in the pass band. These devices are implemented on the size of 1.2 mm × 1.2 mm or 1.85 mm × 1.2 mm for wafer-level packaging using solder-ball bumping.

4. CONCLUSION

In this paper, Cu-based integrated passive devices were fabricated and they showed good RF performance. The RFIPDs in this work have a power handling capability superior to Au-based and Al-based devices. Although the fabricated integrated passive devices were not fully optimized in terms of circuit topology and still need to be improved, low-cost RFIPDs with small-form factor that showed good performances in the microwave region were successfully fabricated and evaluated on 6-in. silicon wafers with our new technology. These integrated passive devices will be the optimal solution for handheld modules and systems where the size or volumetric efficiency is a critical buying criterion.

REFERENCES

1. P. Pieters, S. Brebels, and E. Beyne, Integration of passive components for microwave filters in MCM-D, Multichip Modules Int Conf 1997, pp. 357–362.
2. C.-M. Nam and Y.S. Kwon, High performance planar inductor on oxidized porous silicon (OPS) substrate, IEEE Microwave Guided Wave Lett 7 (1997), 236–238.
3. C.J. Chao, S.C. Wong, C.H. Kao, M.J. Chen, L.Y. Leu, and K.Y. Chiu, Characterization and modeling of on-chip spiral inductors for Si RFICs, IEEE Trans Semiconductor Manuf 15 (2002), 19–29.
4. D.-W. Kim, I.-H. Jeong, H.-S. Sung, T.-O. Kong, J.-S. Lee, C.-M. Nam, and Y.-S. Kwon, High performance RF passive integration on Si smart substrate, IEEE MTT-S Int Symp 2002, pp. 1561–1564.
5. A.C. Reyes, Silicon as microwave substrate, IEDM Tech Dig (1995), 1759–1762.
6. B.K. Kim, B.K. Ko, and K. Lee, Monolithic planar inductor and waveguide substrate on silicon with performance comparable to those in GaAs MMIC, IEDM Tech Dig (1995), 717–720.
7. H.-S. Kim, D. Zheng, A.J. Becker, and Y.-H. Xie, Spiral inductors on Si p/p^{+} substrate with resonant frequency of 20 GHz, IEEE Electron Device Lett 22 (2001), 275–277.